Proceedings of ASME Turbo Expo 2011
GT2011
June 6-10, 2011, Vancouver, British Columbia, Canada

GT2011-46155

INVESTIGATION OF SUBCRITICAL INSTABILITY IN DUCTED PREMIXED FLAMES

Lipika Kabiraj *, **R. I. Sujith**
Department of Aerospace Engineering
Indian Institute of Technology Madras
Chennai-600 0036, India
lipikakabiraj@gmail.com, sujith@iitm.ac.in

ABSTRACT

An experimental investigation of the bistable region of instability in a thermoacoustic system comprising of ducted, premixed laminar flames has been performed. The stability diagram of the system is obtained and the bistable region for a range of flame locations at different fuel-air mixture equivalence ratios is identified. Subsequently, threshold amplitudes for triggering instability in the system using sinusoidal acoustic forcing, introduced externally, is obtained. It is observed that depending on how close the system is to the Hopf point and the nature of oscillations at the Hopf point, the triggered oscillations can exhibit different dynamical behavior.

INTRODUCTION

Thermoacoustic instability is a concern for confined combustion systems such as gas turbines, industrial furnaces and particularly low NOx systems that run on lean premixed combustion. The instability is manifested in the form of high amplitude pressure oscillations that arise due to the establishment of a positive feedback loop between the unsteady heat release rate and the acoustic oscillations within the combustion system, for a certain range of operating conditions. Such oscillations tend to increase the thermal and mechanical loading on the structure of the combustor, greatly reducing the life-span of the combustor [1]. In extreme cases, they can induce violent vibrations within the system, leading to complete failure.

The transition of a thermoacoustic system from steady equilibrium state (fixed point) to an oscillatory state, on variation of operating conditions occurs in two ways - through a supercritical Hopf bifurcation or a subcritical Hopf bifurcation [2]. In the first scenario, there exists a clear demarcation between steady and oscillatory states with respect to the bifurcation or control parameter. The transition from the stable to oscillatory state and vice versa is gradual and occurs exactly at the same parameter value. On the other hand, in the case of a subcritical Hopf bifurcation, as we vary the control parameter, at the critical (Hopf) point, the system jumps from steady equilibrium state to a high amplitude oscillation. While going in the reverse direction, transition back to the steady state does not take place at the Hopf point; the control parameter value needs to be changed further (till the fold point [3]) to restore the steady non-oscillating state of the system. Thus, hysteresis in the system behavior is a manifestation of subcritical Hopf bifurcation [2, 3]. This region of hysteresis is called the subcritical zone or the bistable zone. This bistable zone as we infer from the discussion alone, has two possible states - the steady state that exists when the zone is approached from a stable state and the oscillatory state that exists when the zone is approached from an initially unstable state. At any operating condition, within the bistable zone, it is possible to 'trigger' the system from a stable state to the corresponding oscillatory state, through the introduction of finite amplitude perturbations. This phenomenon is known as triggering instability in the combustion instability parlance [2, 4, 5]. Triggering instability is a concern because the subcritical region, where it occurs, is linearly stable but nonlinearly unstable; i.e. small amplitudes of perturbations will not cause transition but finite amplitudes might trigger instability. Hence, the classical stability analysis and the linear flame transfer function cannot predict triggering instabil-

*Address all correspondence to this author.

ity. In recent investigations, Noiray [6] and Boudy *et al.* [7], have reported, both experimentally and theoretically that using the nonlinear describing function, it is possible to predict various nonlinear characteristics of thermoacoustic systems such as triggering instability, mode switching and hysteresis.

Previous studies reveal that thermoacoustic systems often exhibit subcritical Hopf bifurcation [2,4,8]. Blomshield *et al.* [5] reported the observation of triggering instability during full scale tactical motor stability tests. The susceptibility of a premixed combustor with a swirl stabilized flame, to acoustic disturbances has been investigated by Moeck *et al.* [8] experimentally. They were also able to reproduce the experimental results on triggering and hysteresis through simulations incorporating linear acoustics and a nonlinear response of the flame to upstream air flow rate fluctuations.

Recent efforts to understand and explain the effect of disturbances introduced in the system, in the subcritical zone have revealed that parallels could be drawn between transition of laminar fluid flows to turbulence and triggering of thermoacoustic systems. Balasubramanian and Sujith [9, 10] have shown that non-normality can play an important role in this transition in thermoacoustic systems. Non-normality can cause linear amplification of disturbances leading to transient growth in the system and hence, can trigger the system to self-sustained oscillation even when the disturbance amplitude is small. Juniper [11], based on a dynamical systems approach, gives an analogy between triggering in thermoacoustic systems and bypass transition in fluids [12, 13]. On a simplified Rijke tube model he showed that the amplitudes required for triggering can be small compared to the amplitude of the unstable limit cycle.

Dynamical systems' theory helps in understanding the dynamics of complex systems using geometrical representations. We apply the tools from dynamical systemś theory to a simple thermoacoustic system that consists of ducted, laminar, premixed flames. We study subcritical Hopf bifurcations in such a system, using flame location with respect to the duct as a bifurcation parameter. We examine the asymptotic state of the system, with the specific aim of finding out if the asymptotic state of the system is always a limit cycle, or whether the thermoacoustic system can be triggered to states other than limit cycle. Further, we examine the evolution of the system using phase space analysis, as the system is triggered.

EXPERIMENTAL SETUP

The bifurcation analysis is conducted on a premixed combustor, as depicted in Fig. 1. A multipoint injection burner, similar to the configuration used by Matsui [14] for flame transfer function measurements of premixed, laminar flames, is employed in this study. A similar burner configuration has also been used recently by Noiray [6, 7] for nonlinear flame transfer measurements. The premixed burner has seven conical LPG (Liquefied Petroleum Gas) air premixed flames (A) anchored on a 18 *mm* thick copper block. The top view of the burner is given on the top right of Fig. 1. In preliminary experiments, it was observed that the onset of instability causes flame blowout. In order to facilitate investigation, a fine wire mesh is used to stabilize the flames. The burner tube (C) is 800 *mm* long with an inner diameter of 14 *mm* and thickness of 1.5 *mm*. The burner is connected to a decoupler (D) as shown, which is in turn connected to a premixing chamber (E) for enhanced mixing of the fuel and air. The burner is enclosed in a glass duct (B), 800 *mm* long, closed at the bottom. This glass duct acts as the combustion chamber. During the experiments, the acoustic modes of the duct get coupled with the heat release rate fluctuations leading to self-excited oscillations. The volumetric fuel flow rate ($\mathscr{V}_f$) is kept at 64 *ccm* and 72 *ccm* and the volumetric air flow rate ($\mathscr{V}_a$) at 3700 *ccm*, measured using rotameters with an accuracy of 2%. The corresponding uncertainty in the equivalence ratio is estimated to be around 2.8%. For the results on bifurcation analysis, reported in this paper, two cases, with the equivalence ratio, ϕ, at 0.50 and 0.57, have been studied.

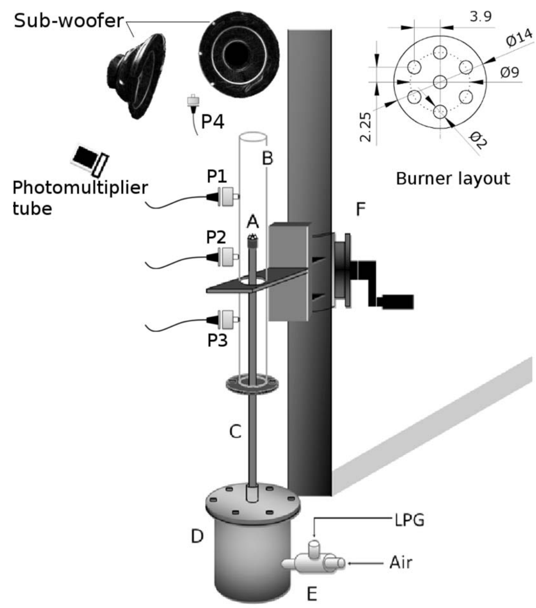

FIGURE 1: SCHEMATIC OF THE SETUP, A-MULTIPLE FLAMES, B-OPEN-CLOSED GLASS DUCT, C-BURNER TUBE, D-DECOUPLER, E-LPG-AIR PREMIXER, F-TRAVERSE, P1, P2, P3 & P4-PRESSURE MICROPHONES. TWO SUB-WOOFERS , ORIENTED TOWARDS THE DUCT OPEN END ARE MOUNTED OUTSIDE THE DUCT FOR EXTERNAL EXCITATION. TOP VIEW OF THE BURNER IS GIVEN AT THE TOP RIGHT CORNER OF THE FIGURE. ALL DIMENSIONS IN *MM*.

Three pressure microphones (model:103B02, PCB piezotronics make), P1, P2 and P3, flush mounted on the walls of the glass duct, as shown in Fig. 1, were installed to monitor the unsteady pressure oscillations. The results reported in this paper are based on pressure time series ($p(t)$) obtained from the microphone P1, which is mounted at a distance of 20 *cm* from the top. A 16-bit analog to digital conversion card (NI-6143) was used for data acquisition which has a resolution of 0.15 mV taking the input voltage range as $\pm 5V$. The uncertainty in pressure microphone measurement is 0.14 *Pa*. Two sub-woofers, driven by an amplifier connected to a function generator, are installed outside the duct, as shown in Fig. 1, for generating acoustic signals. A microphone (P4) is mounted close to the sub-woofers to monitor the generated acoustic signals. The intensity fluctuations ($I(t)$), which are proportional to the heat release rate oscillations in the flame, were detected simultaneously with pressure oscillations using a photomultiplier tube (model no. H5784, Hamamatsu make) equipped with a CH* filter (bandwidth 10 *nm*, centered at 431.4 *nm*). The flame location was measured using a ruler with least count 1 *mm*.

RESULTS AND DISCUSSIONS

We focus primarily on the dynamics of triggered oscillations in the bistable region. Kabiraj *et al.* [15] has shown that the asymptotic states of a thermoacoustic system is not always a limit cycle, but can include quasiperiodic, period doubled or chaotic states. In this study, we examine whether the asymptotic state attained by the thermoacoustic system during the occurrence of triggering instability is always a limit cycle or if the system can be triggered to states other than limit cycle.

We know that it is possible to trigger instabilities in a thermoacoustic system by introducing a perturbation, in the bistable region, with a large enough perturbation. Hence, the perturbation (or the initial condition) given to the system governs the system evolution. However, unfortunately, in experiments, it is often quite difficult to introduce well-determined and controlled initial conditions. As an alternative, in this investigation, we force the system using sinusoidal acoustic forcing at the observed frequency of self-excited limit cycle oscillations at Hopf point of our system ($f = 563.4\ Hz$), for a finite interval of time, in the bistable region. This frequency is close to the second harmonic of a quarter-wave tube with length corresponding to the length of the glass duct used in the experiments.

In subcritical Hopf bifurcation, at the Hopf point, the stable equilibrium fixed point attractor losses its stability and a new branch - an unstable limit cycle is born. This branch is turned backwards and exists before the Hopf point, hence, the term subcritical bifurcation [3]. A saddle-node bifurcation [3, 16] of the unstable limit cycle creates a stable limit cycle branch. This branch can undergo further bifurcations on changing the control parameter gradually, as reported recently by Kabiraj *et al.* [15]. Beyond the Hopf point, all trajectories originating near the fixed point attractor spiral out and settle on the nearest attractor [17]. Hence, we have three attractors in the subcritical zone, a fixed point, a limit cycle and an unstable limit cycle.

In order to identify the bistable region of the system, a stability map of the system is first constructed. The volumetric air flow rate ($\mathscr{V}_a$) is fixed at 3700 *ccm*. Stability of the system is then assessed for all flame location values, and volumetric fuel flow rates ($\mathscr{V}_f$) in the range 56 $ccm - 80$ *ccm*. This corresponds to a lean fuel-air mixture. The range is chosen to maintain well-stabilized conical-shaped flames. The stability diagram of the system is given in Fig. 2. At each fuel-air mixture ratio, the flame location is gradually varied for both increasing and decreasing directions with respect to the open end of the duct. The system is identified as stable if self-sustained oscillations in pressure and intensity measurements are absent. On the other hand, the presence of such oscillations indicates instability. The dark grey shaded region in Fig. 2 marks the linearly unstable regions, where the system is unconditionally unstable. As this region is approached from an initially stable state, oscillations arise spontaneously as the value of the flame location crosses the boundary of this region. The point at which this jump in the behavior of the system is observed, is the linear stability boundary [18] for the system, corresponding to the particular operating condition (the Hopf point, [3]). The light-shaded region is linearly stable, but nonlinearly unstable, as the system is unstable if approached from an unstable state and stable is approached from a stable state. This region, is known as the bistable region as two possible equilibrium states exist - the stable state with no oscillations and an oscillating state which we call unstable. In this paper we conduct experimental analysis of this region and discuss the results from a dynamical systems point of view.

It should be noted that the boundaries drawn are extremely sensitive to changes in the operating parameters, the magnitude of noise in the system and any changes in the system configuration. The aim of the present investigation is to study the system behavior in the bistable region. Establishing the sensitivity of the stability boundaries to noise and constructing a full stability diagram for all possible fuel-air combinations will be a topic of future investigations.

Experiments are performed first at $\mathscr{V}_f = 64$ *ccm*. At a flame location in the bistable region, 5 *mm* from the Hopf point, we introduce acoustic forcing to the system ($f = 563.4\ Hz$), using sub-woofers mounted outside as shown in Fig. 1. This forcing excites a single acoustic duct mode and also the flame surface area oscillations. The system evolution is reported in terms of reconstructed phase portraits [19] from pressure (from microphone P1, Fig. 1) and intensity measurements. Phase portrait is extremely helpful in understanding the evolution of any dynamical system and the embedding theorem [20] enables one to reconstruct the phase portrait from data acquired experimentally. We will discuss briefly about phase space reconstruction from

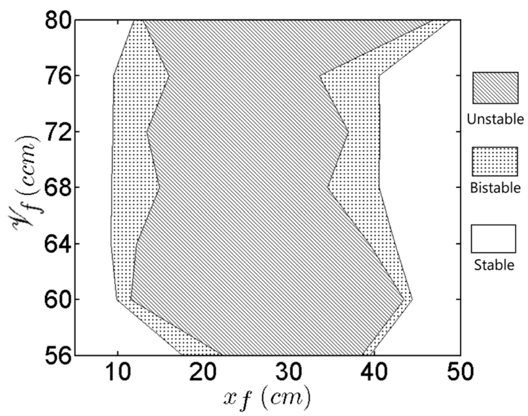

FIGURE 2: STABILITY DIAGRAM OF THE SYSTEM FOR AN AIR FLOW RATE ($\mathscr{V}_a = 3700$ *CCM*). FLAME LOCATION x_f MEASURED FROM THE OPEN END OF THE DUCT. SHADED REGION IS UNSTABLE IRRESPECTIVE OF THE STATE IT IS APPROACHED FROM. DOTTED REGION CORRESPONDS TO THE BISTABLE OR SUBCRITICAL ZONE. OTHER FLAME LOCATIONS ARE STABLE. SYSTEM REMAINS STABLE BEYOND THE RANGE OF FLAME LOCATION VALUES SHOWN IN THE PLOT.

time series data.

The embedding theorem [20] facilitates the construction of multivariate phase space from scalar observations. In experiments, discrete time series sampled at finite intervals of time of a particular variable from the system is available. According to the theorem, it is possible to unfold the geometric structure of the multivariate phase space of the system in a space created out of vectors obtained from the experimental time series. To elaborate, the scalar measurements $s(n),\ n = 1,2,3,\ldots$ can be used to create a vector in d dimensions:

$$\mathbf{y}(n) = [s(n), s(n+\tau), s(n+2\tau), \ldots, s(n+(d-1)\tau)], \quad (1)$$

where $s(n),\ s(n+\tau),\ s(n+2\tau)\ldots$ are called time lagged variables. τ is the time delay and d is the embedding dimension. This vector represents a point in the phase space. The matrix $\mathbf{y}(n)$ gives the coordinates of points in the phase space that represent the reconstructed attractor. We will require a) the time delay (τ) between the vectors and b) the appropriate embedding dimension (d) for representing the actual system in the reconstructed phase space [19, 20]. The details of this technique are not presented here and can be found in [19]. The average mutual information [19] from the time series data and the false nearest neighbor method [19] has been used for each result to get the appropriate time delay (τ) and embedding dimension. All the results reported here have a time delay, $\tau = 5$ and have been reported in a three dimensional space.

Since, the acoustic forcing is applied with frequency same one of the duct acoustic modes (the second harmonic), due to resonance, the pressure amplitude of oscillations within the duct are observed to grow. After a predetermined duration of time, the forcing is stopped and the system evolves on its own. The dynamics of the system then depends on the control parameter value and the amplitude gained by the oscillations by the end of the forcing. If a threshold amplitude is crossed in this process, self-sustained oscillations are set up in the system, otherwise, resonant growth is followed by a decay in the amplitude of oscillations.

To understand subcritical Hopf bifurcation and transition from stable equilibrium state to oscillatory state within the subcritical zone, we will introduce concepts from the dynamical systems theory. From the reconstructed phase space, Fig. 3a, it is seen that the reconstructed trajectories of the system evolve from a steady equilibrium state (fixed point), as marked in Fig. 3, and spirals out towards the inner black loop due to resonant amplification. The inner loop corresponds to the obtained threshold amplitude of oscillations that system needs to cross in order to get triggered. Forcing is discontinued at the time corresponding to the time taken by the trajectories to reach the inner loop. The system evolves on this threshold loop for a while before spiralling out again towards the self-sustained limit cycle state - the outer black loop in Figs. 3a & b. If forcing is ceased earlier, or if it is continued for a longer time, oscillations will decay to the steady state or immediately grow exponentially to the self-sustained state. The same behavior is seen in the phase portrait reconstructed from flame intensity time series (Fig. 3b).

In the case just discussed, the bistable region was found to be limited to 5 *mm* (Fig. 2). This restricts the number of flame locations that can be investigated for triggering. To overcome this limitation, we perform experiments with a different set of operating conditions ($\mathscr{V}_a = 3700$ *ccm*, $\mathscr{V}_f = 72$ *ccm*). The bistable region for this set of operating conditions is wider with respect to the parameter space, allowing us to observe the differences in triggering amplitudes at different flame locations. In addition, self-sustained instabilities that emerge in the system at the Hopf point are period-2 oscillations instead of limit cycle oscillations. The time period of oscillation, for the case of a period-2 oscillation is doubled when compared to limit cycle oscillations (hence, the name period-2). The Fourier spectrum, correspondingly, contains a subharmonic frequency and in the phase space representation, the attractor will be a doubled looped structure. This period-2 oscillation is a result of a period-doubling bifurcation that must have occurred in the parameter space prior to the Hopf point. Further analysis of the bistable region is required to illustrate the system dynamics within this region.

Similar experiments as discussed above are conducted in the bistable region for $\mathscr{V}_f = 72$ *ccm* at four different flame locations in the bistable region. The threshold amplitudes are obtained for each flame location along with the amplitude of triggered oscil-

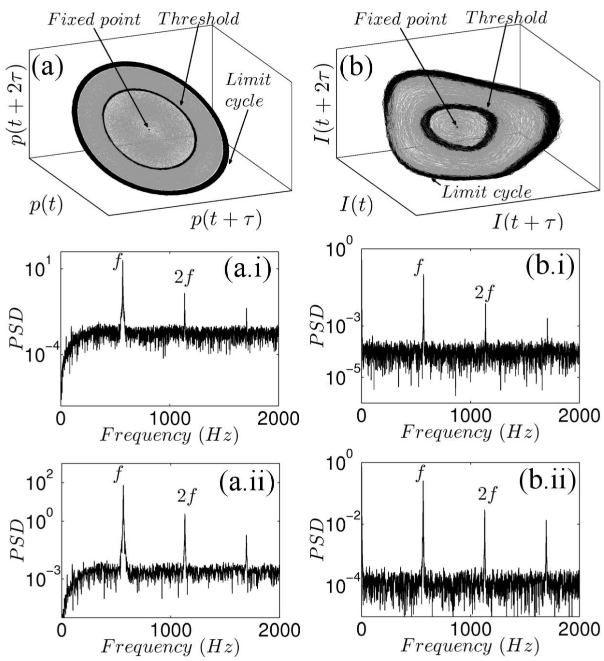

FIGURE 3: TRIGGERING TO LIMIT CYCLE OSCILLATIONS. FIGURES a, a.i AND a.ii CORRESPOND TO PHASE PORTRAIT, POWER SPECTRA AFTER FORCING IS STOPPED AND POWER SPECTRA FOR SELF-SUSTAINED OSCILLATIONS FROM PRESSURE TIME SERIES. FIGURES b, b.i AND b.ii SIMILARLY ARE OBTAINED FROM FLAME INTENSITY TIME SERIES.

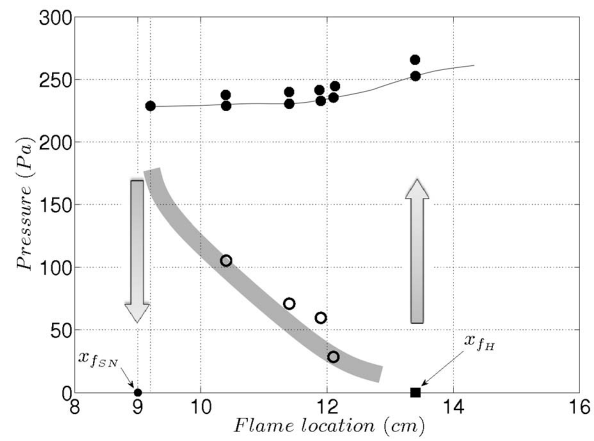

FIGURE 4: BISTABLE REGION FOR $\mathscr{V}_a = 3700$ *CCM* AND $\mathscr{V}_f = 72$ *CCM*. FILLED CIRCLES INDICATE THE AMPLITUDE OF SELF-SUSTAINED OSCILLATIONS. DOUBLE DOTS INDICATE PERIOD-2 OSCILLATIONS. EMPTY CIRCLE REPRESENT THRESHOLD AMPLITUDES REQUIRED FOR TRIGGERING. FILLED RECTANGLE MARKS THE HOPF POINT. HAND DRAWN CURVES CONNECT THE EXPERIMENTALLY OBTAINED POINT. ARROWS INDICATE JUMP IN THE SYSTEM BEHAVIOR.

lations. This information when plotted gives us Fig. 4. As the control parameter (the flame location) is varied, self-sustained oscillations spontaneously arise at the point marked by a filled rectangular marker, x_{f_H} = 13.6 *cm*, the Hopf point, from a set of 20 readings, the standard deviation in the Hopf point location was found to be 0.455 *mm*. In the reverse direction, system jumps to steady non-oscillatory state at flame location, $x_f = x_{f_{SN}}$. This flame location is the point where the saddle-node bifurcation of the unstable limit cycle branch must have occurred. These two points mark the extremities of the bistable region. The arrows indicate a jump in the system behavior. Empty circles in the figure denote the threshold amplitudes obtained at different flame locations and filled circles represent the amplitude of triggered self-sustained oscillations, the two filled circles for each flame location represents the local maxima of the measured pressure time series.

Table 1 gives the threshold amplitudes as a percentage of the triggered oscillations. In Fig. 4, hand drawn curves have been drawn connecting the experimentally obtained points to get an idea of the trend followed by triggering amplitude using resonant forcing. Since, the triggering amplitude cannot be pinpointed exactly, a band has been drawn instead of a sharp line. Furthermore, the triggering amplitude inherently depends on the type of forcing or disturbance given to the system [4].

TABLE 1: THRESHOLD AMPLITUDES FOR TRIGGERING AS GIVEN IN FIG. 5. THE THRESHOLD AMPLITUDE IS STATED AS THE PERCENTAGE OF SELF-SUSTAINED OSCILLATION AMPLITUDE.

Image	Flame Location (x_f)	Threshold amplitude (%)
a	10.4 *cm*	46.0
b	11.4 *cm*	30.8
c	11.9 *cm*	25.6
d	12.1 *cm*	12.1

Time traces from pressure microphone P1 (see Fig. 1) corresponding to triggering at the four flame locations is given in Fig. 5a-d. The grey shaded region in the figure corresponds to the time duration for which sinusoidal resonant forcing is provided. The amplitude of pressure oscillations remains constant

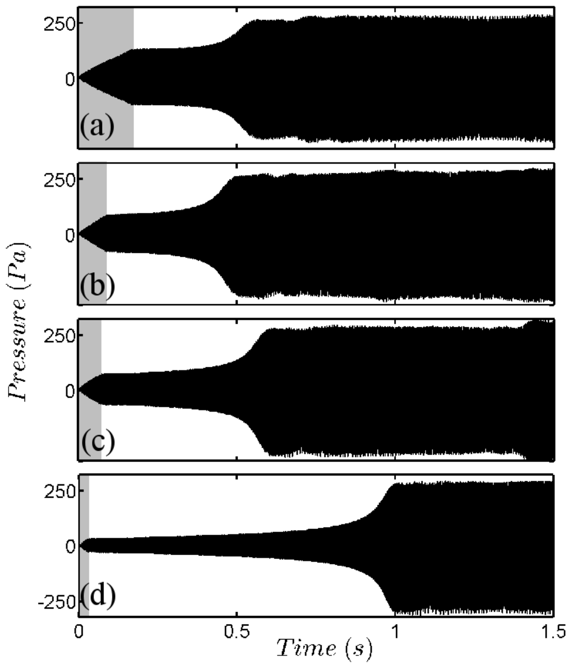

FIGURE 5: PRESSURE TIME SERIES FOR TRIGGERING INSTABILITY VIA RESONANT FORCING AT DIFFERENT FLAME LOCATIONS (REFER TABLE 1). SHADED REGIONS CORRESPOND TO THE DURATION OF FORCING.

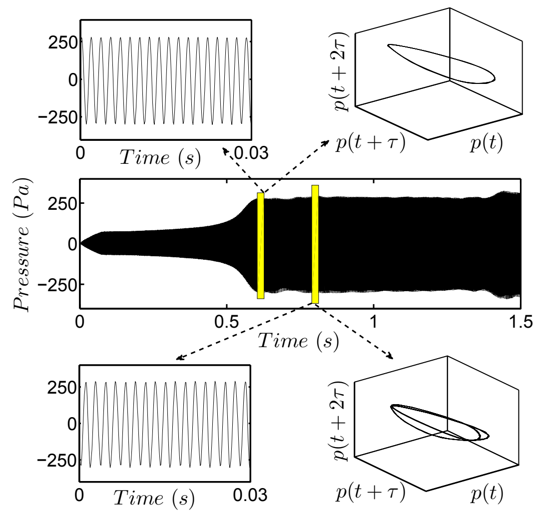

FIGURE 6: DETAILED ANALYSIS OF FIG. 5C. OSCILLATIONS FIRST GET TRIGGERED TO A LIMIT CYCLE STATE AND THEN IMMEDIATELY GOES TO A PERIOD-2 STATE. A, B REPRESENT THE TIME SERIES AND PHASE PORTRAIT OF THE LIMIT CYCLE STATE AND C, D ARE OBTAINED FROM A PERIOD-2 STATE OF THE TRIGGERED OSCILLATIONS. THE THIN HORIZONTAL LINES IN FIGURES A AND C PASS THROUGH THE LOCAL MAXIMA AND MINIMA OF THE SIGNAL. FOR A PERIOD-2 STATE THREE LINES ARE GIVEN INDICATING ONE LOCAL MAXIMA LINES AND TWO LOCAL MINIMA VALUES ARE POSSIBLE.

for a few cycles and grows exponentially towards period-2 oscillations. Reconstructed phase portraits and power spectra corresponding to Fig. 5c are given in Fig. 7. The period-2 nature of triggered oscillations is evident from the power spectra of pressure and intensity time series (Fig. 7a.ii & b.ii) which contains the dominant frequency f and its subharmonic $f/2$. In the phase portraits (Fig. 7a & b) three outer loops are seen. This is because the system first goes to limit cycle oscillations (single loop) and immediately becomes a period-2 oscillations (refer Fig. 6). The frequency component of the signal in Fig. 7a.i & b.i again indicates that system dynamics fills more than two dimensions.

The dynamical properties of a nonlinear system and changes in the dynamics as a result of bifurcations can be studied in a vector space formed by the state variables of the system [16] - the phase space. A system with n degrees of freedom can be represented in an n-dimensional phase space constructed by the state variables . The phase space is filled by trajectories that denote the evolution of the system starting from a point in the phase space - the initial condition in terms of state variables. Every point in the phase space is a possible initial condition. Embedded in this phase space are sets of points called attractors. Trajectories are attracted towards these attractors and eventually evolve on them, once transients have died. Hence, there exists a set of points in the phase space such that trajectories originating from those points settle on one of the attractors present in the phase space. This set forms the basin of attraction for that particular attractor [16]. Figure 8 illustrates the concept of attractors and their basin of attraction in a 3-dimensional phase space. It can be seen that the evolution depends on the direction in which disturbance has been given and the amplitude. If the given disturbance is such that the system has entered the vicinity of the dark region of the Fig. 8, then the system eventually will settle to the attractor A2 and if the disturbance is such that instead of falling in the dark region it falls in the grey region then it eventually settles to the attractor A1. In a real system, there could be other attractors embedded in the phase space. The dark patch in the Fig. 8 is the basin of attraction of the attractor A2 and the grey is the basin of attraction for A1. The boundary which separates the basins of attraction is called basin boundary. The Fig. 4 is the obtained result of the present study which explains that there is existence of more than two attractors in the subcritical zone.

Phase space representation of results as discussed in this sec-

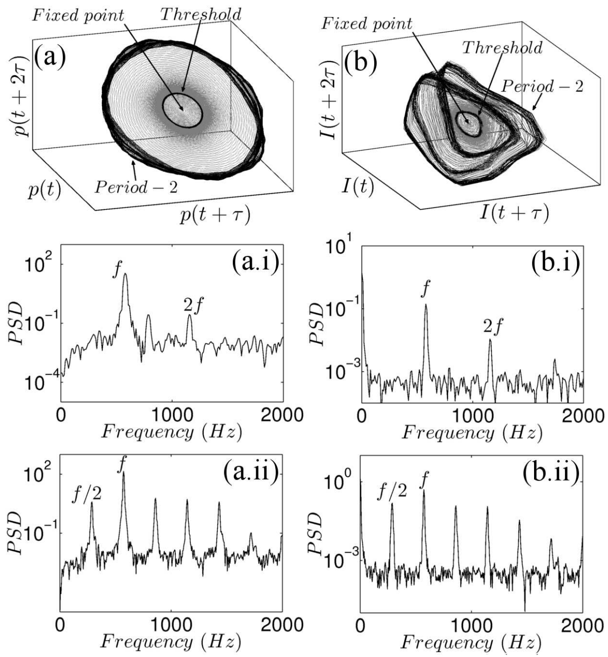

FIGURE 7: TRIGGERING TO PERIOD-2 OSCILLATIONS. FIGURES a, a.i AND a.ii CORRESPOND TO PHASE PORTRAIT, POWER SPECTRA AFTER FORCING IS STOPPED AND POWER SPECTRA FOR SELF-SUSTAINED OSCILLATIONS FROM PRESSURE TIME SERIES. FIGURES b, b.i AND b.ii SIMILARLY ARE OBTAINED FROM FLAME INTENSITY TIME SERIES.

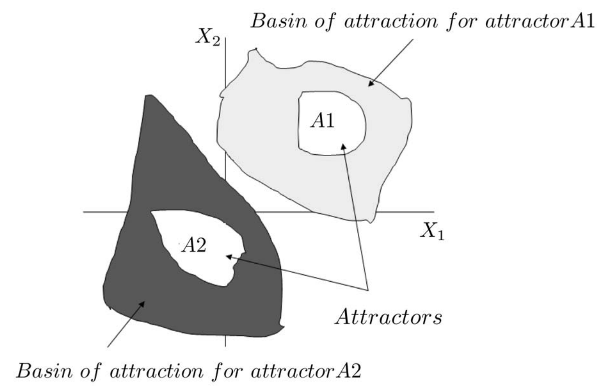

FIGURE 8: A SKETCH OF BASIN OF ATTRACTION IN PHASE SPACE, A1 AND A2 ARE DIFFERENT ATTRACTORS, THEY ARE SURROUNDED BY THEIR OWN BASIN OF ATTRACTION, THE LINE BOUNDING THE EACH BASIN OF ATTRACTION IS CALLED SEPARATRIX. Adapted from Hilborn [17].

tion reveals the interesting dynamics in the bistable region. The extent of the bistable region is highly dependent on the system and the operating conditions. Additionally, the stability boundaries are strongly affected by the presence of noise and other disturbances in the system. Having said that, it is still possible to study the general properties of the bistable region in thermoacoustic systems. For the model thermoacoustic setup discussed here, we observe that for two different operating equivalence ratios, the self-excited oscillations at the Hopf point exhibit two different dynamics - limit cycle and period-2 oscillations. The limit cycle is a result of a subcritical Hopf bifurcation and the period-2 oscillation results from a standard period doubling bifurcation [3,17]. For the same system as discussed here, it is possible that the system undergoes further bifurcations to chaotic oscillations as reported in Kabiraj *et al.* [15]. In practical systems with a higher degrees of freedom and several control parameters, it is expected that such behavior will be more significant and complex.

Another approach of looking at the results is through the idea of basins of attraction. The phase space of the dynamical system as explained above has regions which attract the system dynamics - the attractors, each having its own basin of attraction and a basin boundary. For the results reported here, the system has basins of attraction belonging to three stable attractors namely, the fixed point, limit cycle oscillation and period-2 oscillation. Depending on the operating conditions and amplitude of oscillations present, the system goes to one of the attractors. Again, larger and more complex systems can be expected to have a more complicated phase space structure. This has direct bearing to the implementation of control approaches and the safe operating range of thermoacoustic systems.

Although the structure of the phase space is responsible for the asymptotic states assumed by the system, the transition scenario from a fixed point to another attractor, within the bistable region, is observed to be same for the two different cases seen here. On introduction of the acoustic forcing, the oscillation amplitude grows and depending on the amplitude level at the time forcing is ceased, system goes to a self-excited state or back to the fixed point state. A special case occurs when the amplitude is just at the threshold level. The oscillations then continue at the same amplitude level for a certain time, before growing towards one of the stable attractors (limit cycle or period-2, in the cases presented here).

An analogy could be drawn between the observations in the obtained results and the scenario of bypass transition to turbulence observed in hydrodynamic flows [12,13]. Zinn & Lieuwen [21] (page 19, 2nd paragraph) remarked that "*Although large-amplitude disturbances are generally required to initiate unstable oscillations in nonlinearly unstable systems, a system may be nonlinearly unstable at low-amplitude disturbances that are of* *the order of background noise level. This scenario is somewhat analogous to the hydrodynamic stability of a laminar Poiseuille flow, which is linearly stable but becomes increasingly susceptible to destabilization by nonlinear mechanisms with increasing Reynolds numbers*." For hydrodynamic flows, the basins of attraction of the chaotic attractor, corresponding to turbulence and the fixed point attractor, corresponding to the laminar state are separated by a basin boundary. Similarly, the oscillatory limit cycle state and the fixed point steady state are separated here by an unstable limit cycle. The unstable limit cycle lies on the surface of the basin boundary and is like a separatrix which separates the two basins of attraction [22]. If initial perturbations take the system across the basin boundary, into the basin of attraction of the stable limit cycle oscillations, system evolves to the self-sustained oscillatory state. If the initial condition falls within the basin of attraction of the stable fixed point state, oscillations decay to zero. A similar explanation has been given by Juniper [11] for the occurrence of triggering instability in thermoacoustic systems. In the subcritical region, thermoacoustic systems have two competing attractors - the fixed point and the self-sustained oscillatory state, separated by an $N-1$- dimensional basin boundary surface, where N is the number of degrees of freedom of the system.

The characteristics of the disturbance introduced to the system within the bistable region determines the threshold amplitudes required for triggering in addition to deciding the attractor that attracts the system dynamics. This is in accordance with the above discussion on the basin of attraction. Wicker *et al.* [4] had discussed their numerical analysis on triggering instability in rocket motors with a similar conclusion. This inherent property of dependence on the type of disturbance could be because of the complex structure of the basin boundary. If the basin boundary is a hypersurface enclosing a finite region in the phase space created out of state variables and containing the fixed point attractor, the direction and magnitude of the initial condition vector will determine if the system is taken out of the basin boundary of the fixed point. Depending on the structure of the basin boundary, certain directions might be more favourable (in terms of amplitude required for transition) and hence, a lower magnitude of perturbation will be required when compared to initial conditions in other directions.

In this study, the system is forced using a single frequency acoustic excitation. Equivalently, the phase space representation (Fig. 3 and Fig. 7) shows the evolution to be localised on a plane (a dimensionality of two). Through several experiments we have determined the amplitude which is just enough for the system to evolve to self-sustained oscillations - either a limit cycle or a period-2 oscillation. The frequency of forcing was chosen as the second harmonic of the duct since it was found to be most effective in establishing interaction between flame oscillations and acoustics of the duct. The point where forcing is ceased is the initial condition from where the system evolves on its own. Before getting attracted towards the limit cycle or period-2 oscillation, oscillations stay at a constant amplitude for a certain interval of time (oscillations at the threshold or the inner loops in Fig. 3 a & b and Fig. 7 a & b). The superharmonics observed in the power spectrum while the oscillation is at the threshold amplitude indicate that the dimensionality of the system during that time interval is higher than two. This state corresponds to an unstable attractor towards which the system is initially attracted before going towards a stable attractor. Additionally, the fact that this unstable attractor has a dimension higher than two indicates that the basin boundary is a structure more complicated than a simple loop.

CONCLUSION.

In the present study, experimental investigation of the bistable region in a simple laminar ducted premixed flames, with respect to the flame location has been conducted. Resonant acoustic forcing is used to drive oscillations in the system. The evolution of the system after the external forcing is discontinued is recorded in terms of pressure and heat release rate through flame intensity time series data. In the bistable region for our system, it was observed that instability could be triggered in the system, which is linearly stable, if oscillations are forced beyond certain threshold amplitude.Two cases with different equivalence ratios were chosen for experiments. In the first case, we found that limit cycle oscillations emerged in the system as the control parameter crossed the Hopf point. The triggered oscillations also were limit cycles oscillations. Whereas, in the second case, the self-sustained oscillations at the Hopf point and the triggered oscillations in the bistable region were period-2 oscillations. The threshold amplitudes for triggering thermoacoustic oscillations via resonant acoustic forcing is determined for the latter case for different flame locations and a bifurcation plot for the bistable region is constructed.

This study, if seen from a dynamical systems' perspective, probes into the subcritical zone through a specific section in the phase plane which is determined by the sinusoidal acoustic forcing provided. This forcing takes the system towards the unstable limit cycle which lies on the basin boundary between the fixed point attractor and the stable limit cycle attractor. From the phase space and power spectrum, it is clear that the phase space trajectories evolve on a surface which is closely, but not exactly aligned with the unstable limit cycle loop. In the bistable region as the flame location is changed, the extent of the unstable limit cycle loop changes. The shape and extent of the corresponding basin boundary is also expected to change as the flame location is varied. The basin boundary could be a complex structure, whereas, the unstable limit cycle is a loop on that basin boundary. Investigation in the bistable region by using different shapes of perturbations will help to explore the overall structure of the basin boundary. Further investigations with focus on flame dynamics will help to understand the thermoacoustic interactions in greater detail.

ACKNOWLEDGMENT

This work was funded by the Department of Science and technology, India. The authors gratefully acknowledge discussions with Dr. P. Wahi (IITK, India), J. George and A. Saurabh.

NOMENCLATURE

I Flame intensity fluctuations.
$\mathscr{V}_a$ Volumetric air flow rate, *ccm*.
$\mathscr{V}_f$ Volumetric fuel flow rate, *ccm*.
f Frequency, *Hz*.
p Pressure fluctuations, *Pa*.
ϕ Equivalence ratio.
s General time series.
τ Time delay used for phase space reconstruction.
t Time, *s*.
x_f Flame location, *cm*.

REFERENCES

[1] Suresh, S., 1998. *Fatigue of Materials*. Cambridge University Press.

[2] Lieuwen, T., 2002. "Experimental investigation of limit cycle oscillations in an unstable gas turbine combustor". *Journal of Propulsion and Power,* ***18***(1), February, pp. 61–67.

[3] Strogatz, S. H., 2007. *Nonlinear Dynamics And Chaos: With Applications to Physics, Biology, Chemistry, And Engineering*. Levant Books.

[4] Wicker, J. M., Greene, W. D., Kim, S., and Yang, V., 1996. "Triggering of longitudinal combustion instabilities in rocket motors: Nonlinear combustion response.". *Journal of Propulsion and Power,* ***12***, pp. 1148—-1158.

[5] Blomshield, F. S., Crump, J. E., Mathes, H. B., Stalnaker, R. A., and Beckstead, M. W., 1997. "Stability testing of full-scale tactical motors". *Journal of Propulsion and Power,* ***13***(3), May–June, pp. 349–366.

[6] Noiray, N., Durox, D., Schuller, T., and Candel, S., 2008. "A unified framework for nonlinear combustion instability analysis based on the flame describing function". *Journal of Fluid Mechanics,* ***615***, July, pp. 139–167.

[7] Boudy, F., Durox, D., Schuller, T., and Candel, S., 2011. "Nonlinear mode triggering in a multiple flame combustor.". *Proceedings of the Combustion Institute,* ***33***, pp. 1121 – 1128.

[8] Moeck, J. P., Bothien, M., Schimek, S., Lacarelle, A., and Paschereit, C. O., 2008. "Subcritical thermoacoustic instabilities in a premixed combustor". *14th AIAA/CEAS Aeroacoustics Conference (29th AIAA Aeroacoustics Conference)*, May, pp. 1–18.

[9] Balasubramanian, K., and Sujith, R. I., 2008a. "Thermoacoustic instability in a Rijke tube: non-normality and nonlinearity". *Physics of Fluids,* ***20***, April, pp. 61–67.

[10] Balasubramanian, K., and Sujith, R. I., 2008. "Non-normality and nonlinearity in combustion-acoustic interaction in diffusion flames". *Journal of Fluid Mechanics,* ***594***, pp. 29–57.

[11] Juniper, M. P., 2010. "Triggering in the Rijke tube: non-normality, transient growth and bypass transition". *Journal of Fluid Mechanics in Press*, November, pp. 1–39.

[12] Drazin, P. G., 2002. *Introduction to Hydrodynamic Stability*. Cambridge University Press.

[13] Schmid, P. J., and Henningson, D. S., 2000. *Stability and Transition in Shear Flows*. Springer.

[14] Matsui, Y., 1981. "An experimental study on pyro-acoustic amplification of premixed laminar flames". *Combustion and Flame,* ***43***, June, pp. 199–209.

[15] Kabiraj, L., Saurabh, A., Wahi, P., and Sujith, R. I., 2010. "Experimental study of thermoacoustic instability in ducted premixed flames:periodic, quasi-periodic and chaotic oscillations". *n3l - Int'l Summer School and Workshop on Non-Normal and Nonlinear Effects in Aero- and Thermoacoustics*, May.

[16] Moon, F. C., 2004. *Nonlinear Chaotic and Fractal Dynamics: An Introduction for Applied Scientists and Engineers*. Wiley-VCH Verlag GmbH & Co. KGaA, Weinheim.

[17] Hilborn, R. C., 2000. *Chaos and Nonlinear Dynamics: An Introduction for Scientists and Engineers*. Oxford University Press.

[18] Subramanian, P., Mariappan, S., Sujith, R. I., and Wahi, P., 2010. "Bifurcation analysis of thermoacoustic instability in a horizontal Rijke tube". *International Journal of Spray and Combustion Dynamics,* ***2***, pp. 325–356.

[19] Abarbanel, H. D. I., Brown, R., Sidorowich, J. J., and Tsimring, L. S., 1993. "The analysis of observed chaotic data in physical systems". *Review of Modern Physics,* ***65***(4), October, pp. 167–192.

[20] Ruelle, D., and Takens, F., 1971. "On the nature of turbulence". *Communication in Mathematical Physics,* ***20***(3), pp. 167–192.

[21] Zinn, B. T., and Lieuwen, T. C., 2005. "Combustion instabilities: Basic concepts, Chapter I, combustion instabilities in gas turbine engines: Operational experience, fundamental mechanisms, and modeling". *Progress in Astronautics and Aeronautics, AIAA, Inc,* ***210***, pp. 1–26.

[22] Duguet, Y., Willis, A. P., and Kerswell, R. R., 2008. "Transition in pipe flow: the saddle structure on the boundary of turbulence". *Journal of Fluid Mechanics,* ***613***, June, pp. 255–274.